CHEMISTRY
A EUROPEAN JOURNAL

FULL PAPER

DOI: 10.1002/chem.200((will be filled in by the editorial staff))

Shedding light on the mechanism of CO_2 insertion into Ir(I)-hydroxide and Ir(I)-alkoxide bonds: a kinetic and computational study

Byron J. Truscott,[a] Hedi Kruger,[a] Paul B. Webb,[a,b] Michael Bühl[a] and Steven P. Nolan[a]*

Abstract: We recently reported the facile insertion of CO_2 into Ir(I)-alkoxide and Ir(I)-amide bonds. In particular, [Ir(cod)(I^iPr)(OH)] (I^iPr = 1,3-bis(*iso*propyl)imidazol-2-ylidene) reacted with CO_2 in solution and in the solid state in a matter of minutes to give the novel [{Ir(cod)(I^iPr)}$_2$(μ-κ^1O:κ^2O,O-CO_3)] complex. In the present study we probe this reaction using kinetic and theoretical studies, which enabled us to analyze its facile nature and to fully elucidate the reaction mechanism with excellent correlation between the two methods.

Keywords: carbon dioxide • iridium • mechanistic study •kinetic • DFT• thermodynamic

Introduction

The application of carbon dioxide as a C1 source is not only a strategy towards reduction of greenhouse gases but also presents an opportunity for catalytic development.[1] The employment of CO_2 as a feedstock is still a greatly underdeveloped area of investigation, mainly due to its thermodynamic stability and kinetic inertness,[2] with only a handful of commercial processes in use.[1a, 2-3] Further utilisation of CO_2 is possible only with successful activation of this inert species. Coordination of CO_2 to a metal is often a necessary event for its conversion into useful chemicals.[4] A fundamental understanding of CO_2 coordination is of paramount interest in developing synthetic procedures.[2, 5]

The pioneering work of Vaska[6] and Herskovitz[7] on CO_2 activation using Ir, as well as more recent communications such as those by Morales-Morales[8] and Bergman[9] have identified iridium as a promising candidate in reactions involving CO_2; owing to the numerous coordination modes that the Ir-CO_2 coupling displays.[10] Carbon dioxide insertion into TM-X bonds (where X is an alkoxide or amide) has been well documented from a synthetic perspective[1b, 4, 5d, 11] and several kinetic measurements have been performed on reactions involving CO_2 activation.[12] Although theoretical examinations have been reported, direct comparisons between experimentally derived activation parameters and theoretical calculations are rare.[10, 13] In recent reports by Lee *et al*.,[12d, 12e] the rapid CO_2 insertion into planar [Ni(II)(pyN_2)(OH)]$^-$ (pyN_2 = *N',N'*-(2,6-pyridinedicarboxamidate)) to form Ni-bicarbonate complexes was studied. The authors measured activation parameters by monitoring the reaction using UV/vis spectroscopy and calculated theoretical parameters using DFT methods at the BP86 and B3LYP levels of theory and the compiled experimental and theoretical data were compared in order to provide a mechanistic understanding of the reaction in question.[12d, 12e] Comparative studies such as these are vital, since the limitations of theoretical calculations can be most accurately assessed when compared to experimentally derived results.[4]

Work in our group has focussed on the activation of CO_2, particularly by metal-alkoxides and metal-amides and we recently reported the insertion of CO_2 into Ir(I)-O and Ir(I)-N bonds to form novel Ir(I)-carbonates and Ir(I)-carbamates.[14] Of particular interest was the reaction between CO_2 and [Ir(cod)(I^iPr)(OH)] (**1**), forming the novel dimeric carbonate complex [{Ir(cod)(I^iPr)}$_2$(μ-κ^1O:κ^2O,O-CO_3)] (**2**), (cod = 1,5-cyclooctadiene and I^iPr = 1,3-bis(*iso*propyl)imidazol-2-ylidene) under extremely mild conditions

[a] Dr Byron J. Truscott, Miss Hedi Kruger, Prof. Dr Michael Bühl, Prof. Dr Steven P. Nolan*
EaStCHEM, School of Chemistry,
University of St Andrews,
North Haugh,
St Andrews,
Fife,
KY16 8HE
*E-mail: snolan@st-andrews.ac.uk

[b] Dr Paul B. Webb
Sasol Technology Ltd,
North Haugh,
St Andrews,
Fife,
KY16 8HE

Supporting information for this article is available on the WWW under http://www.chemeurj.org/ or from the author.

(Scheme 1): the reaction proceeds in solution and in the solid state in a matter of minutes under 1 atmosphere of CO_2.

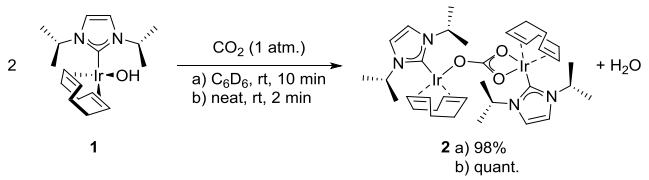

Scheme 1 Reaction between Ir(I)-hydroxide (**1**) and CO_2

Insertion into various Ir(I)-O and Ir(I)-N bonds indicated that a bound heteroatom, bearing a lone-pair, might be essential for the reaction to occur and the lack of activity between CO_2 and a number of Ir(I)-alkyl complexes bearing *sp*-, sp^2- and sp^3-hybridised carbon centres supported this hypothesis.

Based on observed reactivity, we proposed a mechanism for the reaction (Scheme 2).[14] There are a limited number of theoretical investigations into the mechanism of CO_2 insertion into M-X bonds (X = N or O) but reports suggest that the lone-pair on X enables nucleophilic attack on the carbon centre of CO_2[12e, 15] and we envisaged activation by Ir(I)-heteroatom complexes (A) to proceed in the same fashion. Hence, the lone pair on heteroatom X would attack a molecule of CO_2 to deliver the alkoxide, amide or hydroxide to the carbonyl centre *via* a cyclic transition state such as **B**. Furthermore, in the case of XR being a hydroxide, as in complex **1**, a second molecule of Ir(I)-hydroxide would be able to attack the newly formed Ir(I)-bicarbonate complex (C) to release a molecule of water and deliver the dimeric carbonate product **2**.

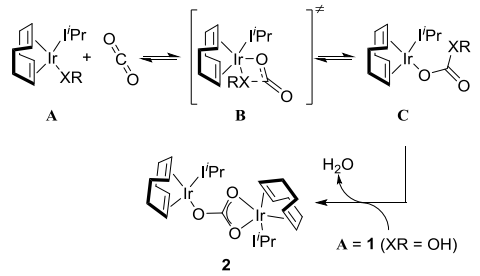

Scheme 2 Proposed mechanism for CO_2 insertion on Ir(I)-hyrdoxide

Results and Discussion

In order to rationalize the reactivity observed between CO_2 and Ir(I)-complexes bearing alkoxide, amide and alkyl moieties, we calculated the driving force for the formation of complex **2** as well as the monomeric carbonate **6** and carbamate **7** from the corresponding Ir(I)-methoxide **3** and Ir(I)-benzylamide **4** respectively (Scheme 3) using DFT methods at the PBE0-D3 level of theory. In addition, the activation of CO_2 by Ir(I)-phenyl complex **5** was computed in order to analyze the lack of reactivity shown by this complex.[16]

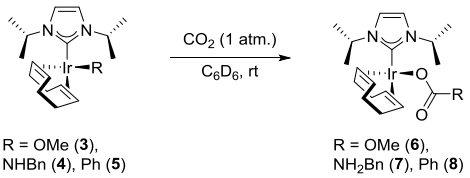

Scheme 3 CO_2 uptake by Ir(I)-alkoxide, -amide and -aryl complexes[14]

Table 1 contains the calculated enthalpies and free energies for carbon dioxide insertion on complexes **1** and **3** – **5**. The computed free energies indicate thermodynamically more stable products in each case. In particular, the computed free energy (and enthalpy) for the formation of **2** (ΔG = -16.28 kcal mol^{-1}, ΔH = -30.88 kcal mol^{-1}, Entry 1) indicates a significantly large thermodynamic driving force for complex **2**.

Table 1 Calculated thermodynamic energies for CO_2 insertion [a]

Entry	Product	ΔH (kcal mol^{-1})	ΔG (kcal mol^{-1})
1	**2**	-30.88	-16.28
2	**6**	-15.37	-4.12
3	**7**	-13.52	-10.21
4	**8**	-16.60	-7.22

[a] PBE0-PCM-D3 (Benzene). See ESI for full calculations of ΔE, ΔH and ΔG using PBEO, PBEO-D3, PBE0-PCM-D3 (DCM) and PBE0-PCM-D3 (Benzene) for each entry.

The reactivity displayed by Ir(I)-hydroxide **1** towards CO_2 to generate the dimeric carbonate, particularly in the solid-state, is unprecedented and we were interested in studying the reaction further. Our primary aim was to test the validity of the proposed mechanism and to shed light on the dimerisation event. However, the nature of the insertion makes it very difficult to isolate potential intermediates such as an Ir(I)-hydrogen carbonate (**C**, Scheme 2). Our approach to the problem was two-fold; firstly we examined the kinetics of the solid-state reaction to determine the activation parameters and secondly, we analysed the reaction profile using DFT methods to identify potential intermediates and transition states. Our goal was to correlate experimentally derived activation energies with theoretical calculations in order to determine the activation barrier and ultimately understand the mechanism at play.

Analysis of the Ir(I)-hydroxide **1** by FTIR revealed that the OH stretch was extremely diagnostic (ν = 3612.7 cm^{-1}). Furthermore, the analysis of **2** showed no distinct bands in this region.[14] Hence, the hydroxide band of **1** provided a perfect spectroscopic handle with which to monitor reaction progress by diffuse reflectance infrared Fourier transform spectroscopy (DRIFTS). **1** (*ca.* 40 mg) was sealed under N_2 in the DRIFTS chamber and a continuous stream of N_2/CO_2 (50:50, 1 atm., 40 mL min^{-1}) was passed over the cell, with reaction progress being monitored *in situ*. Figure 1 shows a series of spectra in the ν(OH) region, collected during the reaction, showing gradual loss of the Ir(I)-hydroxide complex.

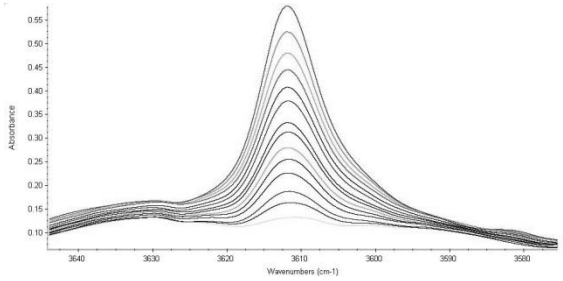

Figure 1 Sample stacked plot of normalised IR data indicating disappearance of the band corresponding to the Ir-hydroxide moiety (ν 3645 – 3577 cm^{-1})

Single beam spectra were ratioed against a background of KBr under the same gas atmosphere. The kinetic trace was then determined by measuring the peak height of the OH band as a function of time, and the reaction was repeated at five different temperatures between 278 K and 358 K (Figure 2). The reaction was studied under a large excess of CO_2 with kinetic traces at different temperatures (Figure 2) indicating pseudo first order behaviour (rate = k_{obs}[**1**]).

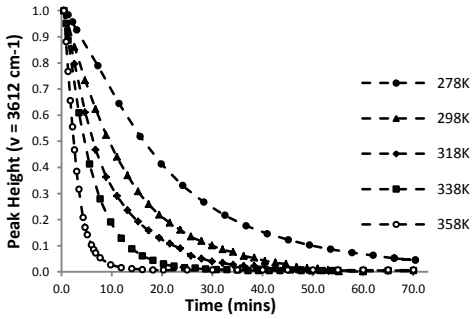

Figure 2 Normalised data showing peak height of IR band corresponding to the Ir-hydroxide moiety (ν = 3612.7 cm^{-1}) vs time at different temperatures (K)

Rate constants were obtained by fitting the kinetic traces to a single exponential using Origin© (see ESI). A linear Eyring plot was obtained with R^2 = 0.9966 (Figure 3) according to the Eyring equation. Activation parameters were calculated as follows: $\Delta H^{\ddagger}$ = 3.6 ± 0.3 kcal mol^{-1}, $\Delta S^{\ddagger}$ = -51.5 ± 0.9 cal K^{-1} mol^{-1} and $\Delta G^{\ddagger}$ (298 K) = 18.9 ± 0.4 kcal mol^{-1}. The results indicate an exergonic process with a small energy barrier to surmount. The large negative entropy value is consistent with an associative transition state involving at least two converging molecules.

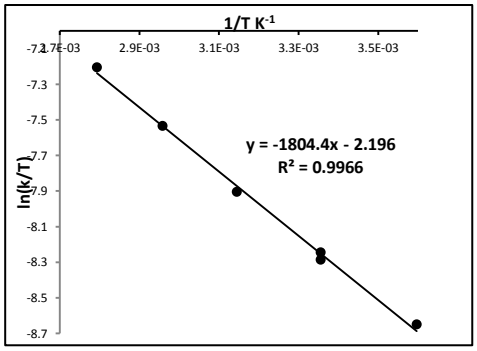

Figure 3 Eyring plot (1/T vs ln(k/T) for reaction between **1** and CO_2 in the solid state.

Following kinetic experiments, we analyzed the reaction pathway at the PBE0-D3 level of theory, with the lowest energy pathway shown in Figure 4. Based on our proposed mechanism, the first step in the reaction was considered to be insertion of CO_2 into the Ir-OH bond to yield an iridium hydrogen carbonate intermediate (**1.3**). An encounter complex was identified as an additional intermediate (**1.2**), formed by the CO_2 approaching **1**. The four-membered transition state between these two intermediates was located, presenting the first reaction barrier (**TS1.2-1.3**, Figure 4). Transformation from **1.2** to **TS1.2-1.3** is accompanied by a decrease in inter-atomic distance between the carbon atom and the oxygen atom of the hydroxide moiety (2.62 to 1.54 Å). More importantly, an elongation of the Ir-O bond from 2.02 Å to 2.17 Å was observed. As expected, the geometry of the CO_2 molecule changes from linear to bent with an O-C-O angle of 139.30° as the Ir-O bond is broken to form the η^1-bicarbonate intermediate (**1.3**). The insertion of CO_2 to form **1.3** is strongly exergonic, such that the enthalpic barrier is essentially insignificant. Hence, the rate limiting step must occur during the encounter with a second molecule of **1** and concomitant elimination of water.

Of the different pathways for dimerisation that were studied, the most favourable one is shown in Figure 4. The interaction between intermediate **1.3** and a second molecule of **1** leads to formation of a tetrahedral diol intermediate **1.4**. From intermediate **1.4**, H_2O elimination occurs *via* an autocatalytic process, whereby an independent H_2O molecule acts as a proton relay in the six-membered transition–state (**TS1.5-2**).

From the results obtained, the rate-limiting step lies somewhere between **1.3** and **TS1.5-2**. The first enthalpic barrier between the two is encountered in the formation of **TS1.3-1.4** ($\Delta H^{\ddagger}$ = 11.06 kcal mol^{-1}) and a second barrier is associated with the formation of **TS1.5-2** ($\Delta H^{\ddagger}$ = 3.47 kcal mol^{-1}, both relative to intermediate **1.3**). At 298 K, the first barrier has a $\Delta G^{\ddagger}$ = 28.30 kcal mol^{-1}, whilst the second shows a $\Delta G^{\ddagger}$ = 29.96 kcal mol^{-1} and largely entropic in nature, in accordance with an associative transition state.

The absolute entropies (and thus the Gibbs free-energy barriers) are strongly overestimated in computations as a result of the ideal-gas approximation made in the standard thermodynamic expressions and the fact that translational entropies in condensed phase tend to be smaller than in the gas phase.[12d, 12e] The activation free energies will suffer from the same over-estimation, particularly in the case of an associative, multi-molecular transformation, where entropy has a larger contribution to the free energy expression than enthalpy. Computed enthalpies are not affected by overestimations of theoretical calculations and Lee *et al.*[12d, 12e] have reported that computed and experimentally derived enthalpies for the CO_2 insertion on Ni(II)-hydroxides differed by only 1 – 2 kcal mol^{-1}, whilst experimental entropies were consistently lower than the theoretical calculations by *ca.* 14 − 17 cal K^{-1} mol^{-1}.[12d, 12e]

The near-quantitative accord between measured and calculated $\Delta H^{\ddagger}$ (3.6 kcal mol^{-1} for formation of **TS1.5-2** from **1.5**) gives us confidence that the DFT-derived pathway in Figure 4 is reasonable. Direct formation of **2** from **1.3** or **1.4** would need to surmount significantly higher barriers (see Figures S15 and S16 in the ESI). This has the interesting implication that a similar autocatalytic mechanism might be dominant in the solid state.[17]

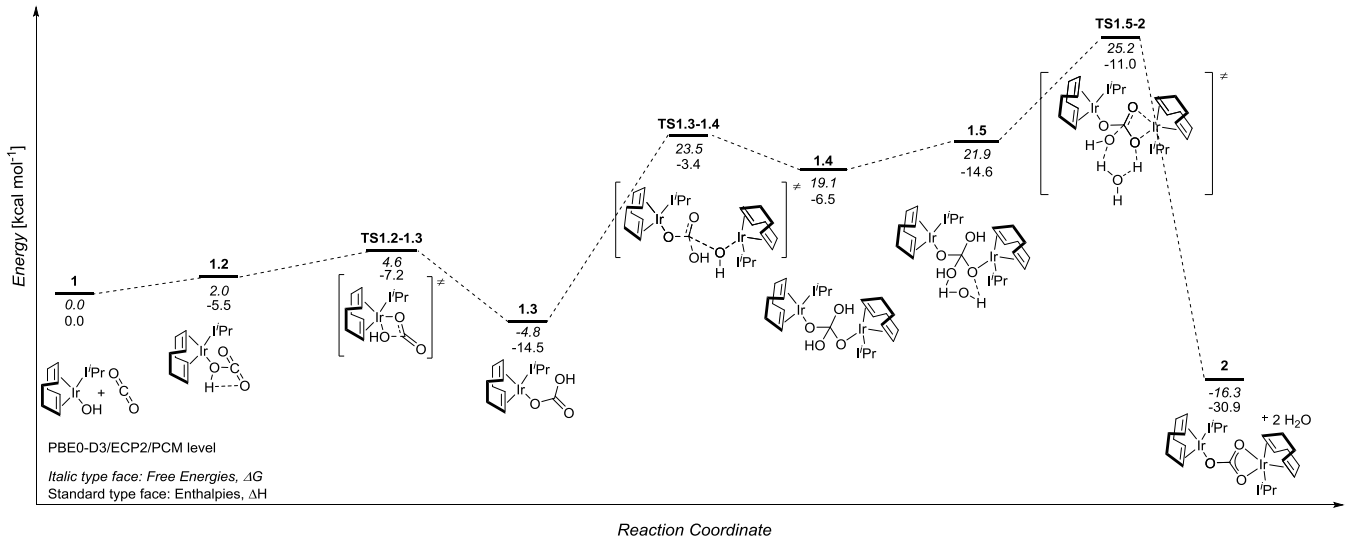

Figure 4 Computed (PBE0-D3 level) reaction profile for CO_2 uptake by **1**

The thermodynamic driving force for the insertion of CO_2 on Ir(I)-OMe **3** to give the Ir(I)-carbonate **6** was calculated as ΔH = -15.37 kcal mol^{-1} and ΔG = -4.12 kcal mol^{-1} (Entry 2, Table 1). The driving force for formation of **6** is comparable with the formation of **1.3** (ΔH = -14.49 kcal mol^{-1} and ΔG = -4.78 kcal mol^{-1}, Figure 4). Figure 5 shows that insertion of CO_2 into the Ir-OMe bond proceeds *via* a 4-membered transition state (**TS3.1-6**), similar to that identified in Figure 4, presenting the largest barrier on both the enthalpy and free energy surface ($\Delta H^{\ddagger}$ = 1.1 kcal mol^{-1} and $\Delta G^{\ddagger}$ = 3.89 kcal mol^{-1} relative to **3.1**). The free energy of activation is highly entropic in nature, with an insignificant barrier on the enthalpy surface, indicating a kinetically favourable reaction, in agreement with experimental results (99% yield after 10 min).[14]. Similar results are obtained for the amide system **4** → **7** (See ESI).

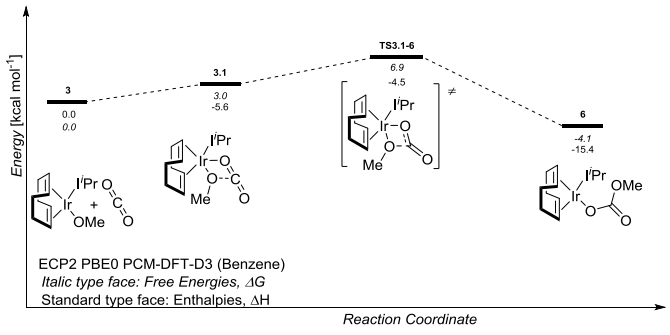

Figure 5 Computed (PBE0-D3 level) reaction profile for CO_2 uptake by **3**

The apparently high driving force for formation of Ir(I)-(OCOPh) **8** from **5** was surprising ($\Delta H^{\ddagger}$ = -16.60 kcal mol^{-1}, $\Delta G^{\ddagger}$ = -7.20 kcal mol^{-1}, Entry 4, Table 1) since all attempts to prepare this complex *via* CO_2 insertion failed, with the Ir(I)-phenyl complex being completely unreactive. Analysis of the reaction profile indicated that although the product is thermodynamically stable, there is a considerable activation barrier to surmount, with formation of the transition state exhibiting a $\Delta H^{\ddagger}$ = 19.54 kcal mol^{-1} and $\Delta G^{\ddagger}$ = 26.02 kcal mol^{-1} relative to intermediate **5.1** (Figure 6). So the reaction is not kinetically favoured.

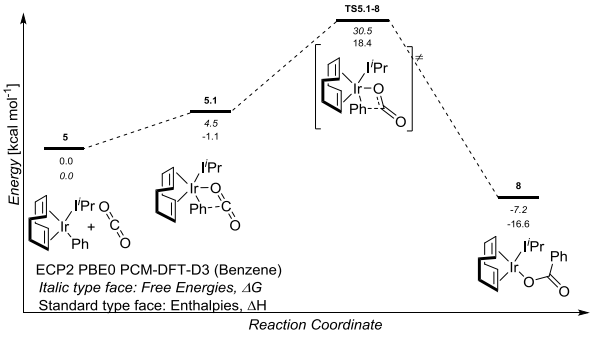

Figure 6 Computed (PBE0-D3 level) reaction profile for CO_2 uptake by **5**

Having developed a mechanistic understanding of the reaction between CO_2 and **1**, we investigated the reaction between CO_2 and an Ir-hydroxide bearing a more bulky NHC ligand to determine if the procedure was general. Hence [Ir(cod)(IPr)(OH)] (**9**)[18] (IPr = 1,3-bis(2,6-di*iso*propylphenyl)imidazol-2-ylidene) was reacted with CO_2 (1 atm), following the reported procedure[14] (Scheme 4). Analysis by $^{13}C\{^1H\}$ NMR spectroscopy indicated that a carbonate complex had indeed formed, with a quaternary carbon resonating at 164.6 ppm (see ESI). However, upon release of the CO_2 atmosphere by bubbling Ar through the reaction mixture, the carbonate complex was converted quantitatively back to starting material (**9**).

While there is no evidence to support an acidic proton by ^1H NMR, (this may be due to strong intermolecular hydrogen bonding) the carbonate signal in the $^{13}C\{^1H\}$ NMR spectrum resonates at a higher field (δ 165 ppm) compared to that of complex **2** (δ 170 ppm).[14] This is diagnostic of a metal bicarbonate structure (**10**, Scheme 4) rather than a carbonate (**11**, Scheme 4).[8, 19] In order to gain further insight into the identity of the product, we performed diffusion ordered NMR spectroscopy (DOSY) experiments on the starting material **9** and the product in solution. The experiments indicated very similar diffusion coefficients in chloroform-*d* (8.37 ±

0.57 x 10^{-10} m^2s^{-1} for **9** and 7.54 ± 0.25 x 10^{-10} m^2s^{-1} for the product). Using the correlation proposed by Morris,[20] we estimated the molecular weight for **9** to be 611 g mol^{-1} (actual MW = 706.01 g mol^{-1}) and that of the product to be 756.8 g mol^{-1} (calculated MW for **10** = 750.2 g mol^{-1}, calculated MW for **11** = 1438.01 g mol^{-1}).

We also analysed the behaviour of **9** under CO_2 in the solid state using DRIFTS. The data clearly shows the consumption of starting material (loss of Ir-OH intensity at ν = 3640 cm^{-1}) and the formation of new bands at 3593, 1720, 1686, 1616, 1281 and 1193 cm^{-1}. When placed under vacuum the newly formed signals deplete and bands associated with the parent recover, indicating the reversible nature of the CO_2 insertion (stacked spectral plots shown in ESI). The presence of a ν(OH) mode at 3593 cm^{-1} suggests that the product of this reaction is in fact bicarbonate rather than carbonate. This is further confirmed by the position of ν(CO) modes, which appear at stretching frequencies that are too high for a carbonate species[8, 21] [22]

Finally, we explored the driving force for formation of **10** and **11** at the PBEO-D3 level of theory, with the energies shown in Scheme 4. While complex **11** appears to be more thermodynamically stable than **10**, it is likely that there is a significant kinetic barrier to overcome between the two species and in the absence of CO_2 the bicarbonate decarboxylates to give the Ir(I)-hydroxide **9** so that there is an equilibrium between the two species.

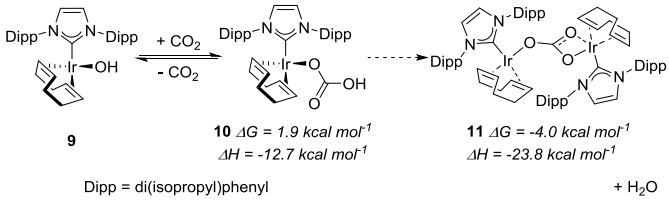

Scheme 4 Reaction between [Ir(cod)(IPr)(OH)] (**9**) and CO_2 and Computed (PBE0-D3 level) energy levels for **10** and **11**

Conclusion

In summary, we have investigated the insertion of CO_2 into Ir(I)-alkoxide bonds. We were particularly interested in the reaction between Ir(I)-hydroxide **1** and CO_2, which gives the [{Ir(cod)(I^iPr)}$_2$-(κ^1O:κ^2 O,O-CO_3)] complex **2**. Determination of activation parameters for the solid state reaction by DRIFTS spectroscopy indicated a pseudo-first order transformation with a small barrier on the enthalpy surface and largely governed by entropy ($\Delta H^{\ddagger}$ = 3.6 ± 0.3 kcal mol^{-1}, $\Delta S^{\ddagger}$ = -51.5 ± 0.9 cal K^{-1} mol^{-1} and $\Delta G^{\ddagger}$ (298 K) = 18.9 ± 0.4 kcal mol^{-1}). DFT calculations identified an auto-catalytic mechanism, whereby the inclusion of an independent H_2O molecule lowers the energy of the transition state in accordance with kinetic calculations. Excellent correlation between the experimentally obtained activation parameters and the theoretical parameters give us confidence that the auto-catalytic process described is dominant, with the implication that a similar mechanism might be operative in the solid state reaction.

DFT calculations have also been performed on the reaction between CO_2 and other Ir(I)-complexes, indicating kinetically and thermodynamically favourable insertion reactions on Ir(I)-methoxide, but not with Ir(I)-alkyl complexes, in accordance with experimental results. Finally, analysis of the reaction between CO_2 and an Ir(I)-hydroxide bearing a bulky NHC ligand indicated that the steric bulk of the NHC has a profound impact on the outcome (and reversibility) of the reaction. The discussions presented in this report are vital to our understanding of CO_2 functionalization by iridium complexes and will enable us to design new strategies for the utilization of CO_2 in our laboratories.

Experimental Section

General Considerations: All manipulations and reactions were performed inside an Argon-filled Inovative Technologies glovebox or on an Argon-supplied Schlenk line unless stated otherwise. All reagents were supplied by Aldrich and used without further purification. [Ir(cod)Cl]$_2$ was provided by Umicore AG. Solvents were distilled and dried as required. NMR data was obtained using a Bruker (^{1}H observe frequency) spectrometer at 303 K in the specified deuterated solvent. All chemical shifts are given in ppm and coupling constants in Hz. Signals on the $^{13}C\{^1H\}$ spectra are singlets unless otherwise stated. Spectra were referenced to residual protonated solvent signals (for ^{1}H) or solvent signals (for ^{13}C): (C_6D_6: ^{1}H δ 7.16 ppm, ^{13}C δ 128.06 ppm; CD_2Cl_2: ^{1}H δ 5.32 ppm, ^{13}C δ 53.84 ppm, $CDCl_3$: ^{1}H δ 7.25 ppm, ^{13}C δ 77.23 ppm). All known compounds were prepared according to reported procedures.[14, 18]

[Ir(cod)(IPr)(CO_3H)] (10): A J-Young type NMR tube was charged with [Ir(cod)(IPr)(OH)] (**9**) (25 mg, 0.035 mmol) in C_6D_6 (0.6 mL). The sample was frozen in liquid N_2 and the Ar atmosphere was removed *in vacuo*. The sample was allowed to thaw before CO_2 (*ca.* 1 atm.) was added, and the reaction mixture was agitated for at least 10 mins before NMR analysis was conducted**. ^{1}H NMR** (300 MHz, C_6D_6): δ 7.29 (t, 5H, $^3J_{HH}$ = 7.6, Ar-H), 7.24 – 7.17 (m, 7H, Ar-H), 6.53 (s, 4H, N-(C*H*)$_2$-N), 5.51 – 5.38 (m, 4H, cod-CH), 3.01 – 2.89 (m, 4H, cod-CH), 1.76 – 1.39 (m, 40H, cod-CH_2, CH_3), 1.33 – 1.16 (m, 8H, cod-CH_2), 1.04 (d, 24H, $^3J_{HH}$ = 6.7, CH_3). **$^{13}C\{^1H\}$ NMR** (125 MHz, CD_2Cl_2): δ 184.7 (Ir-$C_{carbene}$), 164.6 (CO_3H), 147.1 (ArC), 136.2 (N-ArC), 130.2 (ArCH), 130.0 (ArCH), 124.3 (N-(*C*H)$_2$-N), 123.9 (ArCH), 83.7 (cod-CH), 46.7 (cod-CH), 33.3 (*C*H(CH_3)$_2$), 29.4 (cod-CH_2), 29.0 (cod-CH_2), 26.8 (CH_3), 22.8 (CH_3). DRIFTS ν = 3593(s, OH), 1720(s, CO), 1686(s, CO), 1616(w), 1281(s, CO) and 1193(s, CO) cm^{-1}.

Kinetic Experiments: Kinetic measurements were performed in the solid state using a low temperature DRIFTS chamber (Harrick). Ir-hydroxide (*ca.* 40 mg) was loaded into the chamber, which was then purged with N_2 (50 mL min^{-1}) for *ca.* 30 minutes. The chamber was then heated or cooled to the desired reaction temperature and isolated using ball valves situated at the inlet and outlet lines. The gas inlet line was then purged with a mixture of N_2 and CO_2 (1:1, 1 atm, 40 mL min^{-1} combined). During the collection of a data series (Nicolet Nexus FTIR spectrometer, 4 cm^{-1} resolution, 32 scans per spectrum) the N_2/CO_2 gas stream was passed through the chamber at 40 mL min^{-1}. Single beam spectra were ratioed against a background of KBr under the same gas atmosphere. Kinetic traces were then determined by measurement of the peak height of the OH stretch of Ir-OH as a function of time.

DFT Calculations: Geometry optimisation and frequency calculations were performed at the PBE0/ECP1 level, i.e. employing the hybrid version of the PBE functional,[23] the Stuttgart-Dresden pseudopotential on Ir with its associated valence basis (SDD),[24] and 6-31G* basis for all remaining atoms. Further polarization functions were employed on O-bonded hydrogen atoms. This and comparable levels have performed very well in describing structural parameters of 5d-metal complexes.[25] Using these optimized structures (which are collected in the ESI), single point calculations were performed at the PBE0-D3/ECP2 level, i.e. using the same functional and SDD pseudopotential as before, 6-31G* basis set for all atoms of the N-heterocyclic carbene ligands, 6-311+G** basis elsewhere, and three-body dispersion corrections according to *Grimme*[26] Inclusion of dispersion is necessary in order to determine accurate energies.[27] These single point calculations also used the Polarizable Continuum Model (PCM) in its integral equation formalism variant (IEF-PCM) to model the effect of solvents,[28] employing the parameters of benzene. These energies were corrected to enthalpies and Gibbs free energies using standard statistical thermodynamics expressions and the harmonic vibrational frequencies calculated at the PBE0/ECP1 level (at standard temperature and pressure). Transition states were fully optimized following constrained pre-optimizations, scans of the potential energy surface along suitable coordinates, or

using the QST3 interpolation method,[29] and were confirmed by Intrinsic Reaction Coordinate (IRC) calculations. All calculations were performed using Gaussian 09.[30]

Acknowledgements

The ERC (Advanced Researcher Award FUNCAT to SPN), the EPSRC and Sasol technology (Stipend to BJT) are gratefully acknowledged for support. Umicore AG are thanked for their generous gift of materials. SPN is a Royal Society Wolfson Award holder. PBW holds a Royal Society Industry Fellowship. MB thanks the School of Chemistry and EaStCHEM for support and for access to a computer cluster maintained by Dr H. Früchtl. Thank you to Dr Tomas Lebl for assistance with NMR studies.

[1] a) W. Wang, S. Wang, X. Ma, J. Gong, *Chem. Soc. Rev.* **2011**, *40*, 3703-3727; b) A. Behr, *Angew. Chem. Int. Ed.* **1988**, *27*, 661-678.

[2] X. Yin, J. R. Moss, *Coord. Chem. Rev.* **1999**, *181*, 27-59.

[3] a) M. Aresta, A. Dibenedetto, *J. Mol. Catal. A: Chem.* **2002**, *182–183*, 399-409; b) M. Aresta, A. Dibenedetto, *Dalton Trans* **2007**, 2975-2992.

[4] T. Fan, X. Chen, Z. Lin, *Chem. Commun.* **2012**, *48*, 10808-10828.

[5] a) T. Sakakura, J.-C. Choi, H. Yasuda, *Chem. Rev.* **2007**, *107*, 2365-2387; b) D. H. Gibson, *Chem. Rev.* **1996**, *96*, 2063-2096; c) A. M. Appel, J. E. Bercaw, A. B. Bocarsly, H. Dobbek, D. L. DuBois, M. Dupuis, J. G. Ferry, E. Fujita, R. Hille, P. J. A. Kenis, C. A. Kerfeld, R. H. Morris, C. H. F. Peden, A. R. Portis, S. W. Ragsdale, T. B. Rauchfuss, J. N. H. Reek, L. C. Seefeldt, R. K. Thauer, G. L. Waldrop, *Chem. Rev.* **2013**, *113*, 6621-6658; d) W. Leitner, *Coord. Chem. Rev.* **1996**, *153*, 257-284.

[6] B. R. Flynn, L. Vaska, *J. Am. Chem. Soc.* **1973**, *95*, 5081-5083.

[7] a) T. Herskovitz, L. J. Guggenberger, *J. Am. Chem. Soc.* **1976**, *98*, 1615-1616; b) T. Herskovitz, *J. Am. Chem. Soc.* **1977**, *99*, 2391-2392.

[8] D. W. Lee, C. M. Jensen, D. Morales-Morales, *Organometallics* **2003**, *22*, 4744-4749.

[9] T. A. Hanna, A. M. Baranger, R. G. Bergman, *J. Am. Chem. Soc.* **1995**, *117*, 11363-11364.

[10] F. J. Fernández-Alvarez, M. Iglesias, L. A. Oro, V. Polo, *Chem. Cat. Chem.* **2013**, *5*, 3481-3494.

[11] K. K. Pandey, *Coord. Chem. Rev.* **1995**, *140*, 37-114.

[12] a) S. Schindler, C. D. Hubbard, R. van Eldik, *Chem. Soc. Rev.* **1998**, *27*, 387-393; b) E. Fujita, R. van Eldik, *Inorg. Chem.* **1998**, *37*, 360-362; c) D. J. Darensbourg, E. B. Frantz, *Inorg. Chem.* **2008**, *47*, 4977-4987; d) D. Huang, O. V. Makhlynets, L. L. Tan, S. C. Lee, E. V. Rybak-Akimova, R. H. Holm, *Inorg. Chem.* **2011**, *50*, 10070-10081; e) D. Huang, O. V. Makhlynets, L. L. Tan, S. C. Lee, E. V. Rybak-Akimova, R. H. Holm, *P. Natl. Acad. Sci. U S A* **2011**, *108*, 1222-1227.

[13] R. V. Chaudhari, A. Seayad, S. Jayasree, *Catal. Today* **2001**, *66*, 371-380.

[14] B. J. Truscott, D. J. Nelson, A. M. Z. Slawin, S. P. Nolan, *Chem. Commun.* **2014**, *50*, 286-288.

[15] a) S. Sakaki, Y. Musashi, *Inorg. Chem.* **1995**, *34*, 1914-1923; b) T. J. Schmeier, A. Nova, N. Hazari, F. Maseras, *Chem. - Eur. J.* **2012**, *18*, 6915-6927.

[16] Complex **8** has previously been reported by us via reaction between **1** and benzoic acid. See ref 18

[17] Complexes **1** and **2** are prepared under anhydrous conditions. Therefore, H_2O is either present as vapour in the CO_2 and/or it comes from the reaction itself.

[18] B. J. Truscott, D. J. Nelson, C. Lujan, A. M. Z. Slawin, S. P. Nolan, *Chem. - Eur. J.* **2013**, *19*, 7904-7916.

[19] L. M. Martínez-Prieto, C. Real, E. Ávila, E. Álvarez, P. Palma, J. Cámpora, *Eur. J. Inorg. Chem.* **2013**, *2013*, 5555-5566.

[20] R. Evans, Z. Deng, A. K. Rogerson, A. S. McLachlan, J. J. Richards, M. Nilsson, G. A. Morris, *Angew. Chem. Int. Ed.* **2013**, *52*, 3199-3202.

[21] a) T. Yoshida, D. L. Thorn, T. Okano, J. A. Ibers, S. Otsuka, *J. Am. Chem. Soc.* **1979**, *101*, 4212-4221; b) A. J. Edwards, S. Elipe, M. A. Esteruelas, F. J. Lahoz, L. A. Oro, C. Valero, *Organometallics* **1997**, *16*, 3828-3836.

[22] a) K. Nakamoto, Y. A. Sarma, H. Ogoshi, *The Journal of Chemical Physics* **1965**, *43*, 1177-1181; b) C. Su, D. L. Suarez, *Clays Clay Miner.* **1997**, *45*, 814-825.

[23] a) J. P. Perdew, K. Burke and M. Enzerhof, *Phys. Rev. Lett.*, **1996**, *77*, 3865. b) Adamo, C.; Barone, V. *J. Chem. Phys.* **1999**, *110*, 6158.

[24] M. Dolg, H. Stoll, H. Preuss and R.M. Pitzer, *J. Phys. Chem. A*, **1993**, *97*, 5852.

[25] M. Bühl, C. Reimann, D. A. Pantazis, T. Bredow, F. Neese, *J. Chem. Theory Comput.* **2008**, *4*, 1449.

[26] S. Grimme, J. Antony, S. Ehrlich and H. Krieg, *J. Chem. Phys.*, **2010**, *132*, 154104.

[27] See e.g.: a) K. K. Pandey, S. K. Patadir, P. Patidar, R. Wishwakarma and P. K. Barwiya., *Anorg. Allg. Chem.*, **2014**, *640*, 370. b) S. Grimme, *WIREs Comput. Mol. Sci.*, **2011**, *1*, 211. c) W. Hujo and S. Grimme, *J. Chem. Theory Comput.*, **2013**, *9*, 308. d) S. Ehrlich, J. Moellmann and S. Grimme, *Acc. Chem. Res.*, **2013**, *46*, 916.

[28] a) J. Tomasi, B. Mennucci and R. Cammi, *Chem. Rev.*, **2005**, *105*, 2999. b) B. Mennucci and J. Tomasi, *J. Chem. Phys.*, **1997**, *106*, 5151. c) V. Barone, M. Cossi and J. Tomasi, *J. Comp. Chem.*, **1998**, *19*, 404.

[29] C. Chen, S. F. Shyu and F.S. Hsu, *International Journal of Quantum Chemistry*, **1999**, *74*, 395.

[30] Gaussian 09, Revision **D.01**, M. J. Frisch, G. W. Trucks, H. B. Schlegel, G. E. Scuseria, M. A. Robb, J. R. Cheeseman, G. Scalmani, V. Barone, B. Mennucci, G. A. Petersson, H. Nakatsuji, M. Caricato, X. Li, H. P. Hratchian, A. F. Izmaylov, J. Bloino, G. Zheng, J. L. Sonnenberg, M. Hada, M. Ehara, K. Toyota, R. Fukuda, J. Hasegawa, M. Ishida, T. Nakajima, Y. Honda, O. Kitao, H. Nakai, T. Vreven, J. A. Montgomery, Jr., J. E. Peralta, F. Ogliaro, M. Bearpark, J. J. Heyd, E. Brothers, K. N. Kudin, V. N. Staroverov, R. Kobayashi, J. Normand, K. Raghavachari, A. Rendell, J. C. Burant, S. S. Iyengar, J. Tomasi, M. Cossi, N. Rega, J. M. Millam, M. Klene, J. E. Knox, J. B. Cross, V. Bakken, C. Adamo, J. Jaramillo, R. Gomperts, R. E. Stratmann, O. Yazyev, A. J. Austin, R. Cammi, C. Pomelli, J. W. Ochterski, R. L. Martin, K. Morokuma, V. G. Zakrzewski, G. A. Voth, P. Salvador, J. J. Dannenberg, S. Dapprich, A. D. Daniels, Ö. Farkas, J. B. Foresman, J. V. Ortiz, J. Cioslowski, and D. J. Fox, Gaussian, Inc., Wallingford CT, **2009**

Received: ((will be filled in by the editorial staff))
Revised: ((will be filled in by the editorial staff))
Published online: ((will be filled in by the editorial staff))

CO_2 Fixation

Byron J. Truscott,[a] Hedi Kruger,[a] Paul B. Webb,[b] Michael Bühl[a] and Steven P. Nolan[a]…* Page – Page

Shedding light on the mechanism of CO_2 insertion into Ir(I)-hydroxide and Ir(I)-alkoxide bonds: a kinetic and computational study

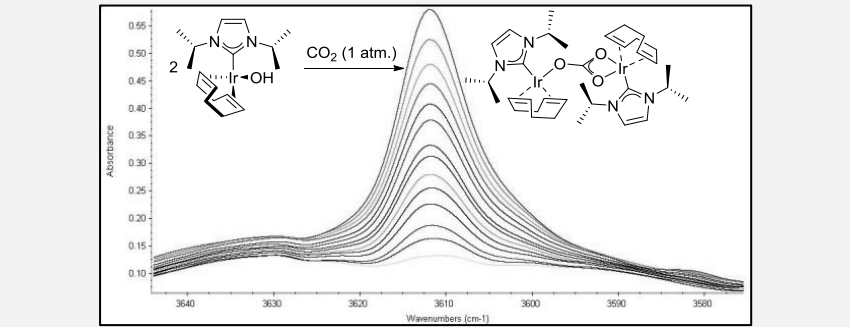

The insertion of CO_2 into Ir(I)-alkoxide bonds is examined from both a kinetic and thermodynamic perspective. The two methods showed excellent correlation, shedding much needed light on the mechanism of CO_2 fixation by Ir(I)-complexes.